Imiquimod-Induced Psoriasis-Like Skin Inflammation in Mice Is Mediated via the IL-23/IL-17 Axis[1]

Leslie van der Fits,[2]*† Sabine Mourits,*† Jane S. A. Voerman,† Marius Kant,*† Louis Boon,§ Jon D. Laman,† Ferry Cornelissen,†‡ Anne-Marie Mus,†‡ Edwin Florencia,*† Errol P. Prens,[3]*† and Erik Lubberts[3]†‡

Topical application of imiquimod (IMQ), a TLR7/8 ligand and potent immune activator, can induce and exacerbate psoriasis, a chronic inflammatory skin disorder. Recently, a crucial role was proposed for the IL-23/IL-17 axis in psoriasis. We hypothesized that IMQ-induced dermatitis in mice can serve as a model for the analysis of pathogenic mechanisms in psoriasis-like dermatitis and assessed its IL-23/IL-17 axis dependency. Daily application of IMQ on mouse back skin induced inflamed scaly skin lesions resembling plaque type psoriasis. These lesions showed increased epidermal proliferation, abnormal differentiation, epidermal accumulation of neutrophils in microabcesses, neoangiogenesis, and infiltrates consisting of $CD4^+$ T cells, $CD11c^+$ dendritic cells, and plasmacytoid dendritic cells. IMQ induced epidermal expression of IL-23, IL-17A, and IL-17F, as well as an increase in splenic Th17 cells. IMQ-induced dermatitis was partially dependent on the presence of T cells, whereas disease development was almost completely blocked in mice deficient for IL-23 or the IL-17 receptor, demonstrating a pivotal role of the IL-23/IL-17 axis. In conclusion, the sole application of the innate TLR7/8 ligand IMQ rapidly induces a dermatitis closely resembling human psoriasis, critically dependent on the IL-23/IL-17 axis. This rapid and convenient model allows further elucidation of pathogenic mechanisms and evaluation of new therapies in psoriasis. *The Journal of Immunology,* **2009, 182: 5836–5845.**

Imiquimod (IMQ),[4] a ligand for TLR7 and TLR8 and a potent immune activator, is used for topical treatment of genital and perianal warts caused by human papilloma virus (1). The clinical indications have additionally been expanded to include treatment of other virus-associated skin abnormalities as well as (pre)cancerous skin lesions such as actinic keratoses and superficial basal cell carcinomas (2, 3). IMQ can exacerbate psoriasis in patients with a well-controlled psoriasis during topical treatment of actinic keratoses and superficial basal cell carcinomas (4–7). IMQ-induced exacerbation of psoriasis occurs at both the treated area and, interestingly, also at distant skin sites that were previously unaffected (5–7). Furthermore suggestive for systemic effects of topical IMQ application are our own clinical observations that patients with IMQ-induced psoriasis at distant body sites exhibit flu-like symptoms (unpublished data). Important hallmarks of IMQ-induced psoriasis are the infiltration of plasmacytoid dendritic cells (pDC) and type I IFN activity (4). Accordingly, application of IMQ on mouse skin leads to rapid influx of pDC (8).

The antiviral and antitumor effects of IMQ are mostly mediated via activation of TLR7 and TLR8 expressed by monocytes, macrophages, and pDC (reviewed in Ref. 9). Thereby, the production of proinflammatory cytokines and chemokines is increased, directly resulting in antiviral activity mediated by IFN-α and in influx of immune cells to the site of application. Topical application of IMQ induces migration of Langerhans cells (LC) from the treated skin into the draining lymph nodes (10). Furthermore, IMQ stimulates maturation of pDC (11) and can induce profound Th1 responses (12). Stimulation of keratinocytes by IMQ results in increased cytokine production (13, 14), although other reports showed a lack of TLR7/8 expression on human keratinocytes (15, 16), and consequently no response to the IMQ analogs loxoribine and R-848 (15). In addition to TLR-dependent activity of IMQ, TLR-independent effects of IMQ have been described. IMQ can interfere with adenosine receptor signaling, augmenting inflammation and thereby acting synergistically with the primary, TLR-dependent mode of action (17).

In the past much progress was made in elucidating the pathological mechanisms of psoriasis, and consequently also in the development of novel therapeutic options. However, this progress is hampered by the lack of a convenient and rapid mouse model for psoriasis, representing most features of the human psoriatic lesion. One of the most elegant models is the xenograft model, in which immunodeficient mice are transplanted with human psoriasis-prone skin (18, 19). These experiments are laborious and expensive, and require considerable expertise and technical skills. Furthermore, the lack of a functional immune system in this xenograft model limits its use in the study of immune intervention approaches.

Recently, it was postulated that IL-23, a cytokine driving the development of IL-17- and IL-22-producing Th17 cells, is functionally involved in the pathogenesis of psoriasis. Expression of IL-23 is increased in psoriasis lesional skin (20, 21), and increased numbers of Th17 cells are present (22). Intradermal injection of

Departments of *Dermatology, †Immunology, and ‡Rheumatology, Erasmus Medical Center, Rotterdam, The Netherlands; and §Bioceros BV, Utrecht, The Netherlands

Received for publication September 11, 2008. Accepted for publication February 23, 2009.

The costs of publication of this article were defrayed in part by the payment of page charges. This article must therefore be hereby marked *advertisement* in accordance with 18 U.S.C. Section 1734 solely to indicate this fact.

[1] J.S.A.V. and J.D.L. are supported by the Dutch MS Research Foundation. F.C., A.-M.M., and E.L. are supported by the Dutch Arthritis Foundation.

[2] Address correspondence and reprint requests to Dr. Leslie van der Fits, Department of Dermatology, Room T02-32, Leiden University Medical Center, P.O. Box 9600, 2300 RC Leiden, The Netherlands. E-mail address: L.vanderfits@lumc.nl

[3] E.P.P. and E.L. contributed equally to this work.

[4] Abbreviations used in this paper: IMQ, imiquimod; DETC, $\gamma\delta$-positive dendritic epidermal T cells; KO, knockout; LC, Langerhans cells; pDC, plasmacytoid dendritic cells; WT, wild type.

www.jimmunol.org/cgi/doi/10.4049/jimmunol.0802999

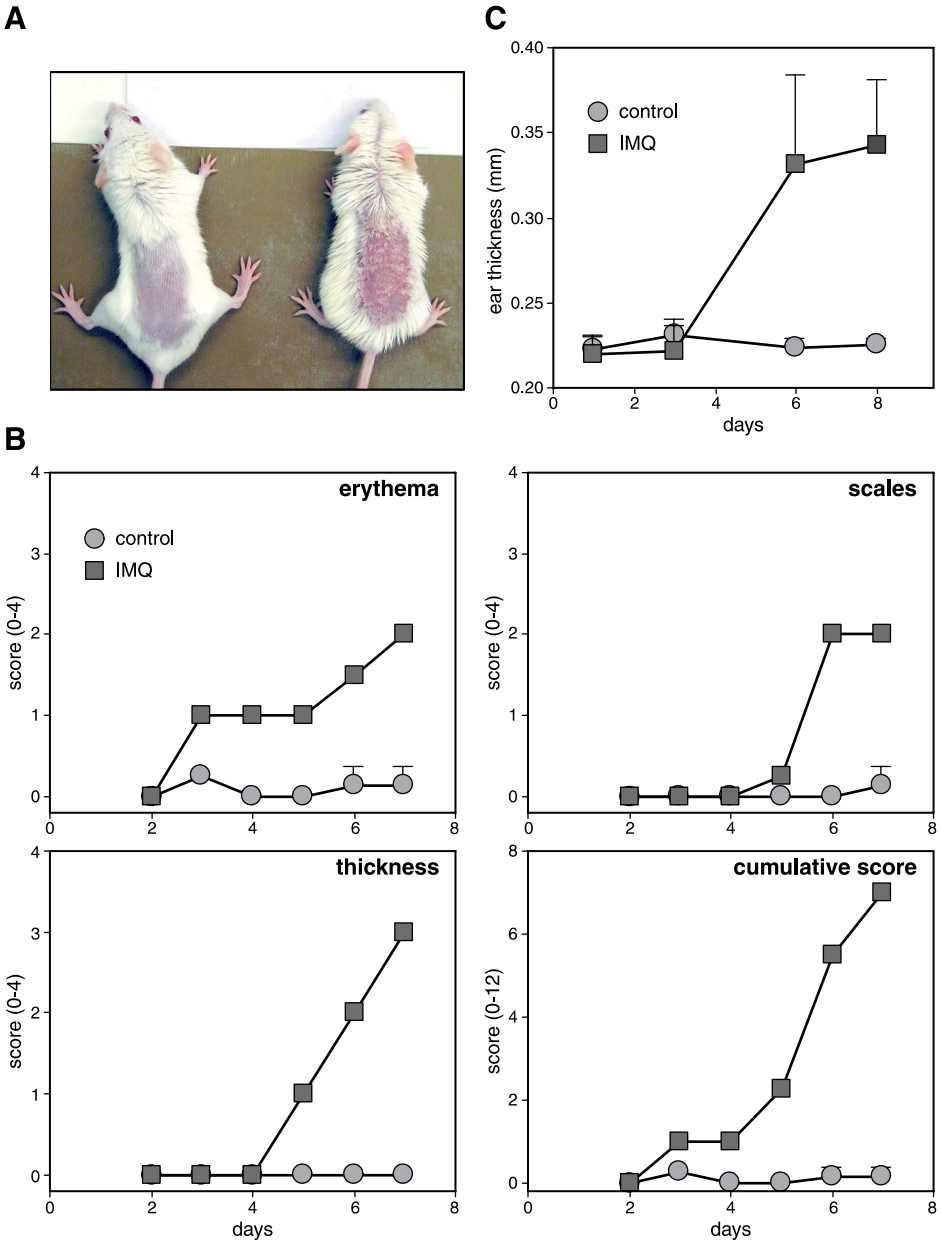

FIGURE 1. IMQ-induced skin inflammation in mice phenotypically resembles psoriasis. BALB/c mice were treated daily with IMQ cream or control cream on the shaved back skin and right ear. *A*, Phenotypical presentation of mouse back skin after 6 days of treatment. *B*, Erythema, scaling, and thickness of the back skin was scored daily on a scale from 0 to 4. Additionally, the cumulative score (erythema plus scaling plus thickness) is depicted. Symbols indicate mean score ± SD of four mice per group. *C*, Ear thickness of the right ear was measured on the days indicated. Symbols represent mean ear thickness ± SD for four mice per group. The experiment shown is representative of >12 experiments.

IL-23 in mouse skin resulted in erythema, a mixed inflammatory infiltrate and epidermal hyperplasia (23, 24). A mAb against the p40 subunit shared by IL-12 and IL-23 shows therapeutic efficacy in psoriasis (25). In patients with psoriasis, amelioration of psoriasis is associated with reduced Th17 responses (26, 27). In addition to an important role for adaptive immunity in psoriasis development, the involvement of innate immunity in the pathogenesis of psoriasis was postulated previously (28). This role was recently confirmed and exemplified by the strong correlation between psoriasis and a higher genomic copy number for β-defensin genes (29).

Application of IMQ on mouse skin results in the influx of various cells of the immune system, as well as hyperplasia of the epidermis (8). This prompted us to assess whether IMQ-induced skin inflammation in mice provides a bona fide model representing most features of human psoriasis, thereby focusing on the involvement of the IL-23/IL-17 axis. Our data show that IMQ-induced dermatitis in mice closely resembles human psoriasis lesions in terms of the phenotypic and histological characteristics, and that lesion development is critically dependent on IL-23 and IL-17.

Materials and Methods

Mice and treatments

Mice (BALB/c, C57BL/6) were purchased from Harlan. IL-23p19-deficient (IL-23p19 knockout (KO)) breeding pairs were kindly provided by Dr. Ghilardi (Genentech) (30) and bred in-house. Mice deficient for IL-17RA (IL-17RA KO) were kindly provided by Dr. J. Tocker (Amgen) (31) and bred in-house. Immunodeficient mice lacking both RAG2 and the common γ-chain (RAG2$^{-/-}$common $\gamma^{-/-}$), backcrossed on a BALB/c background, have been described previously (32). Mice were kept under specific pathogen-free conditions and provided with food and water ad libitum. All experiments were approved by the animal ethics committee according to Dutch legislation on animal experiments.

Mice at 8 to 11 wk of age received a daily topical dose of 62.5 mg of commercially available IMQ cream (5%) (Aldara; 3M Pharmaceuticals) on the shaved back and the right ear for 5 or 6 consecutive days, translating in a daily dose of 3.125 mg of the active compound. This dose was empirically determined to cause most optimal and reproducible skin inflammation in mice (data not shown). Control mice were treated similarly with a control vehicle cream (Vaseline Lanette cream; Fagron).

CD3$^+$ cells were depleted by injection of the mice with 400 μg/mouse rat-anti-mouse CD3 mAb 17A2 (33) on days −3, 0, and 3, relative to the start of IMQ application.

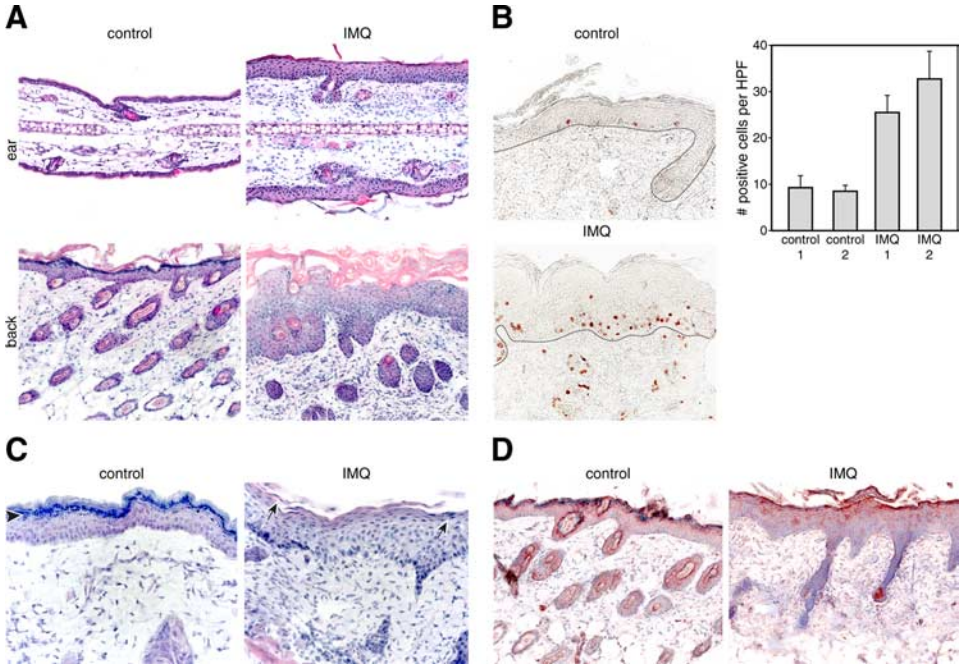

FIGURE 2. IMQ treatment alters keratinocyte proliferation and differentiation. Mice were treated for 6 days with IMQ or control cream. *A*, H&E staining of the ear and back skin of mice. *B*, Two mice per group were injected with BrdU 2 h before sacrifice. BrdU incorporation in keratinocytes in the back skin was detected by immunohistochemistry (*left panel*). A dashed line indicates the epidermis/dermis boundary. Bars in the right panel represent mean number of BrdU positive cells ± SD in four representative high-power fields (HPF) in individual mice treated with control cream or IMQ. *C*, A higher magnification of H&E sections of the back skin. Retention of nuclei in the stratum corneum of IMQ-treated mice is indicated with arrows, and the stratum granulosum is marked with an arrowhead. *D*, Immunohistochemical analysis of the keratinocyte differentiation marker involucrin in back skin.

Scoring severity of skin inflammation

To score the severity of inflammation of the back skin, an objective scoring system was developed based on the clinical Psoriasis Area and Severity Index (PASI), except that for the mouse model the affected skin area is not taken into account in the overall score. Erythema, scaling, and thickening were scored independently on a scale from 0 to 4: 0, none; 1, slight; 2, moderate; 3, marked; 4, very marked. The level of erythema was scored using a scoring table with red taints. The cumulative score (erythema plus scaling plus thickening) served as a measure of the severity of inflammation (scale 0–12).

At the days indicated, the ear thickness of the right ear was measured in duplicate using a micrometer (Mitutoyo).

Immunohistochemistry

Samples from back and ear skin (3 mm diameter) were immersed in TissueTek (Bayer), snap-frozen in liquid nitrogen, and stored at −80°C until use. Six-micrometer cryosections of snap-frozen skin were cut using a cryostat (Jung Frigocut 2800 E; Leica). Sections were fixed in acetone (Fluka Chemie) containing 0.5% H_2O_2 for 10 min at room temperature. Staining was performed essentially as described previously (34). Slides were incubated overnight at 4°C, or for 1 h at room temperature, with primary Abs against the following Ags or cell types: CD3 (clone KT3), CD4 (GK1.5), CD8 (YTS169), CD11c (N418), MHC-II (M5/114), Gr1/Ly6G (RB6-8C5), involucrin (PRB-140C), pDC (120G8), macrophages (ER-MP23), and endothelial cells (MECA-20). This was followed by incubation for 30 min with biotin-linked secondary donkey-anti-rabbit, goat-anti-hamster, or rabbit-anti-rat Abs and peroxidase-linked avidin (Dako). 3-Amino-9-ethylcarbazole (Sigma-Aldrich) was used as the chromogen, resulting in a bright red staining. Sections incubated with an Ab of the same isotype as the specific Ab but of irrelevant specificity served as controls.

Quantification of the stainings was performed by two researchers for two sections of two mice per group in two independent experiments. Numbers of cells positive for 120G8 (pDC), MHC-II (APC), CD3 (all T cells), CD4 (Th cells), and CD8 (CTLs) were counted per section or per high power field (HPF). Semiquantitative scoring for CD11c (DC), ER-MP23 (macrophages), and Gr1 (granulocytes) was performed, on a scale from 0 to 3 (0, negative; 1, <20 positive cells/HPF; 2, 20–100 positive cells/HPF; 3, >100 positive cells/HPF).

Keratinocyte proliferation was determined by BrdU incorporation. Mice were injected with 1 mg of BrdU 2 h before sacrifice. Back skin was fixed in 4% paraformaldehyde and embedded in paraffin. Sections were deparaffinized and boiled in 5 mM citrate buffer (pH 5.5). Sections were incubated with mouse-anti-BrdU (Dako), followed by HRP-labeled goat-anti-mouse IgG. HRP activity was visualized using 3-amino-9-ethylcarbazole (Sigma-Aldrich) as the chromogen.

Flow cytometry

Spleen samples were minced through a 70-μm mesh to obtain single-cell suspensions. Cells were washed twice, and 2×10^6 cells per staining were fluorescently labeled by incubation for 10 min at room temperature with the following mAbs diluted in PBS/0.2% BSA: FITC-conjugated anti-CD3, PE-conjugated anti-CD4, allophycocyanin-conjugated anti-CD8, PE-conjugated CD11c, allophycocyanin-conjugated B220, allophycocyanin-conjugated CD11b (all from BD Pharmingen), FITC-conjugated 120G8 (35), or FITC-conjugated F4/80 (Caltag Laboratories).

For intracellular detection of cytokines, 2×10^6 spleen cells/ml were stimulated with plate-bound anti-CD3 mAb (clone 145-2C11 (BD Pharmingen), 10 μg/ml in PBS) in the presence of GolgiStop (BD Biosciences) for 4 h. Cells were harvested and stained with anti-CD4 or anti-CD8 mAbs (BD Biosciences), followed by intracellular staining using mAbs PE-conjugated anti-IL-17A, allophycocyanin-conjugated anti-IFN-γ, and PE-conjugated anti-IL-4 (all from BD Pharmingen) after fixation and permeabilization with 2% paraformaldehyde and 0.5% saponin.

Samples were acquired on a flow cytometer (FACScan or FACSCalibur; BD Biosciences) and analyzed using CellQuest software (BD Biosciences). Viability of the cells was checked by staining with propidium iodide, or based on forward and side scatter patterns.

Real-time quantitative PCR

Total mRNA was extracted from whole biopsies from the back skin isolated after sacrificing the mice using the GeneElute Mammalian Total RNA kit (Sigma-Aldrich). Using 1 μg of total RNA template, cDNA was prepared using SuperScript II reverse transcriptase (Invitrogen) and oligo(dT) and random hexamer primers.

IL-17A, IL-17F, IL-22, IL-23, and GAPDH mRNA levels were measured by real-time quantitative PCR analysis using the ABI PRISM 7700 sequence detection system (Applied Biosystems). PCR primers were spanning at least one intron/exon boundary. Sequences for the PCR primers, and reference numbers for probes (Universal Probe Library; Roche Applied Science), were: IL-17A, forward primer, 5′-TTT TCA GCA AGG AAT GTG GA, reverse primer, 5′-TTC ATT GTG GAG GGC AGA C, probe no. 34; IL-17F, forward primer, 5′-CAA GAA ATC CTG GTC CTT CG, reverse primer, 5′-GAG CAT CTT CTC CAA CCT GAA, probe no. 45; IL-22, forward primer, 5′-TTT CCT GAC CAA ACT CAG CA, reverse primer, 5′-CTG GAT GTT CTG GTC GTC AC, probe no. 17; IL-23, forward primer, 5′-CAC CTC CCT ACT AGG ACT CAG C, reverse primer, 5′-TGG GCA TCT GTT GGG TCT, probe no. 25; GAPDH, forward primer, 5′-TCC ACT GGC GTC TTC AC, reverse primer, 5′-GGC AGA GAT GAT GAC CCT TTT, probe no. 9. Cytokine and GAPDH levels were calculated relative to amounts found in a standard sample, and

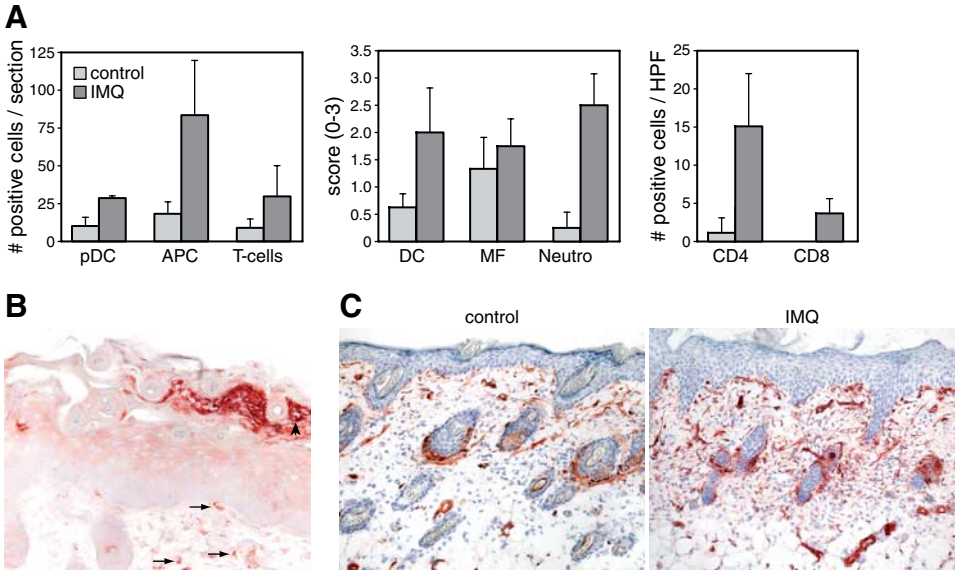

FIGURE 3. IMQ treatment results in accumulation of T cells, neutrophils, and APC, as well as neoangiogenesis. Back skin was analyzed by immunohistochemistry. *A*, Composition of the leukocyte infiltrate was analyzed using the markers 120G8 (pDC), MHC-II (APC), CD3 (T cells), CD11c (DC), ER-MP23 (macrophages, MF), Gr1 (neutrophils), CD4 (Th cells), and CD8 (CTLs). Numbers of pDC, APC, and T cells were counted per section or per high-power field (HPF), and semiquantitative scoring for DC, macrophages, and neutrophils was performed. Scoring was performed by two independent researchers on two mice per group. A representative experiment is shown. *B*, Accumulation of $Gr1^+$ cells just beneath and in the stratum corneum is indicated with an arrowhead. Additionally, scattered $Gr1^+$ cells are detected in the dermis (arrows). *C*, Neoangiogenesis was visualized by the Ab MECA20, which recognizes endothelial cells.

cytokine levels were corrected for GAPDH mRNA levels to normalize for RNA input.

Results

Structural features of IMQ-induced skin inflammation in mice

To assess whether topical IMQ application induces skin inflammation accompanied by structural features characteristic for psoriasis, we applied IMQ cream on the shaved back skin and right ear of BALB/c mice for 6 consecutive days. Two or 3 days after the start of IMQ application, the back skin of the mice started to display signs of erythema, scaling, and thickening. A typical example is shown in Fig. 1*A*. The independent scores in a representative experiment are depicted in Fig. 1*B*. From days 2–3 onward, inflammation was visible, which continually increased in severity up to the end of the experiment. Mice shaved and treated daily with control cream did not show any sign of inflammation. The scores of individual mice in every group were consistently very similar over a large number of independent experiments, resulting in the typically minimal SDs in Fig. 1*B*. As an independent parameter of skin inflammation, we measured ear thickness in mice. Daily treatment of the right ear of the mice led to significant increases in ear thickness that were measurable from days 5–6 onward (Fig. 1*C*).

IMQ treatment results in increased proliferation and altered differentiation of keratinocytes

Analysis of H&E-stained sections from the IMQ-treated skin showed increased epidermal thickening in back and ear skin (Fig. 2*A*). This acanthosis was caused by hyperproliferation of keratinocytes, as increased numbers of keratinocytes in the basal cell

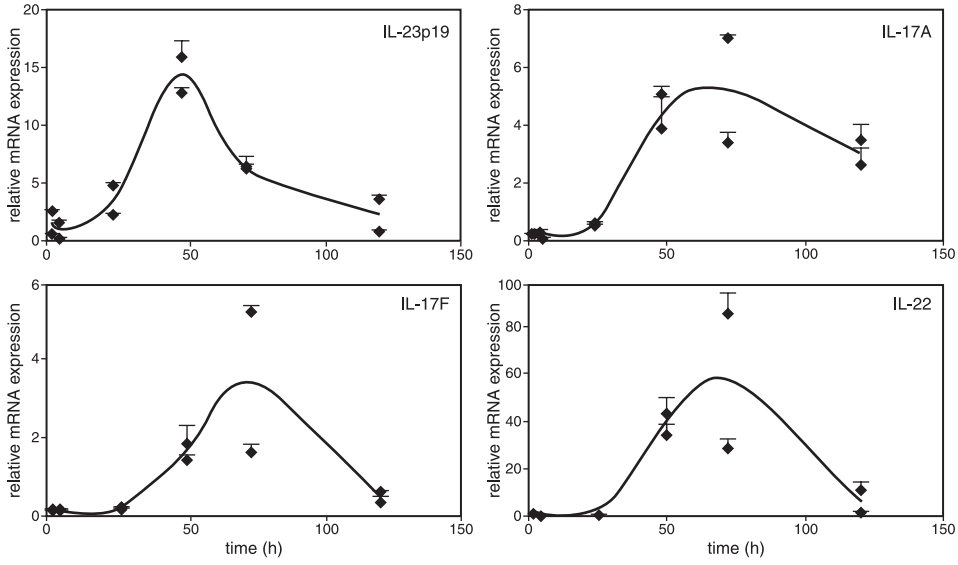

FIGURE 4. IMQ transiently induces cytokines of the IL-23/IL-17 axis in skin. Mice were treated daily with IMQ or control cream and sacrificed at the time points indicated. RNA was extracted from back skin, and expression of IL-22, IL-23p19, IL-17A, and IL-17F was determined by quantitative RT-PCR. Each symbol represents mRNA expression relative to GAPDH mRNA levels in an individual mouse, and the average value between the duplicate mice is indicated with a line.

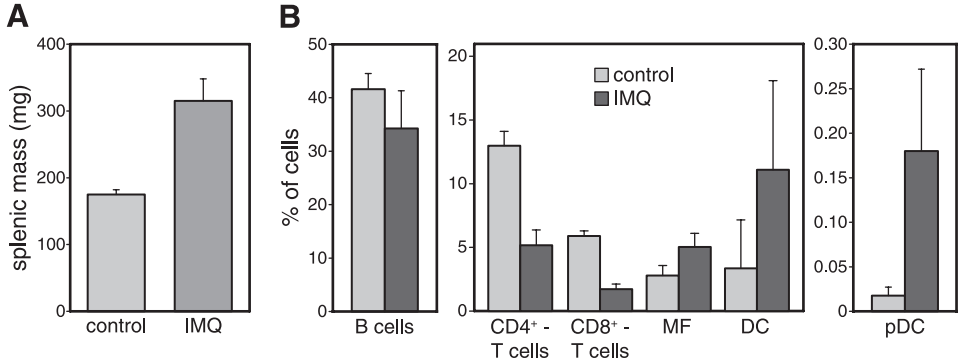

FIGURE 5. Topical IMQ increases spleen mass and alters its cellular composition. Mice were treated with IMQ or control cream for 6 consecutive days. *A*, Mice were sacrificed and spleen mass was determined. *B*, Spleen cells were analyzed for the percentage of B cells ($B220^+120G8^-$), T cells ($CD3^+CD4^+CD8^-$ or $CD3^+CD4^-CD8^+$), macrophages (MF; $F4/80^+CD11b^+CD11c^-$), DC ($CD11b^+CD11c^{high}$), and pDC ($120G8^+CD11c^{int}B220^+$) by flow cytometry. Bars represent mean percentage of positive cells ± SD of four mice per group in a representative experiment out of two to five experiments.

layer showed BrdU incorporation (Fig. 2*B*). Scaling of the skin is often an indication of parakeratosis, that is, altered epidermal differentiation, a phenomenon typical for psoriasis skin lesions. Close examination of H&E-stained sections of back skin showed retention of nuclei in the stratum corneum of IMQ-treated mice (indicated with arrows in Fig. 2*C*). Furthermore, the granular layer, as observed in control-treated mice (arrowheads in Fig. 2*C*), was absent in IMQ-treated mice. Involucrin, a marker of terminal keratinocyte differentiation, showed typical expression in the upper stratum spinosum of the epidermis of control-treated mice, whereas IMQ treatment resulted in involucrin expression spread more throughout the epidermis (Fig. 2*D*).

In summary, IMQ treatment results in hyperproliferative keratinocytes and a disturbed epidermal differentiation (parakeratosis) as demonstrated by the retention of nuclei in the stratum corneum, the absence of a granular layer, and an altered involucrin expression pattern, all of which match the characteristic histological picture of plaque type psoriasis.

The inflammatory infiltrate in IMQ-treated skin is composed of T cells, APC, pDC, and neutrophils

In the H&E sections of IMQ-treated back and ear skin, abundant infiltrates of mononuclear cells were observed. Immunohistochemical staining revealed that these infiltrates consisted of increased numbers of APC in general, as defined by MHC class II expression, and the specialized APC subsets of dermal DC and pDC. Additionally, T cells and neutrophils were present (Fig. 3*A*). In contrast, numbers of macrophages in IMQ-treated skin were not significantly altered when compared with control-treated skin (Fig. 3*A*). In IMQ-treated skin, accumulations of neutrophils ($Gr1^+$ cells) were observed just beneath the stratum corneum (Fig. 3*B*), highly comparable to Munro microabscesses in psoriasis skin lesions. Furthermore, IMQ-treated skin showed increased vascularization, as visualized by immunohistochemical staining using MECA-20 as a marker for endothelial blood vessels (Fig. 3*C*).

In conclusion, immunohistochemical analysis of IMQ-induced dermatitis reveals many similarities with human psoriasis with respect to the composition of the inflammatory infiltrate and neoangiogenesis.

Transient increase in proinflammatory cytokines of the IL-23/IL-17 axis in IMQ-treated skin

A role for the IL-23/IL-17 axis in the development of psoriasis has been demonstrated previously. To assess the involvement of this axis in the development of IMQ-induced dermatitis in mice, we first determined gene expression levels of cytokines playing a pivotal role in this system. BALB/c mice were treated daily with IMQ, sacrificed after 1.5, 4, 24, 48, 72, and 120 h, and mRNA expression of cytokines in the skin was determined by quantitative RT-PCR analysis. A transient increase in IL-23p19 mRNA expression was observed, with a maximum expression after 48 h (Fig. 4). This increase was followed by induction of expression of IL-17A, IL-17F, and IL-22, all showing maximum expression after 72 h, and declining afterward (Fig. 4). Thus, expression of cytokines of the IL-23/IL-17 axis is increased by IMQ. This induction is transient, despite continuous IMQ treatment and continuing increase in disease severity (Fig. 1*B*).

IMQ induces splenomegaly with increased numbers of Th17 cells

At the end of the experiments after 5 to 6 days of IMQ treatment, we consistently found a significant spleen enlargement with an increase in weight of ~2-fold (Fig. 5*A*). Cellular composition of the spleens of control- and IMQ-treated mice was determined by flow cytometry. No obvious differences were

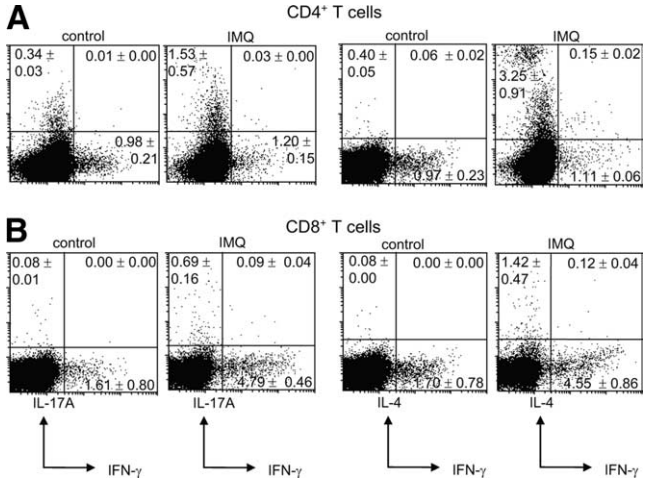

FIGURE 6. Topical IMQ increases percentages of splenic Th17 cells. Mice were treated with IMQ or control cream for 6 consecutive days. Splenic cells were isolated, in vitro stimulated for 4 h by plate-bound anti-CD3, and analyzed by flow cytometry for intracellular IL-17A, IFN-γ, and IL-4 expression. Cells were gated for $CD4^+$ (*A*) or $CD8^+$ (*B*). A representative example is shown. Numbers indicate the mean percentage of cells ± SD present within a quadrant ($n = 2$ mice/group).

observed in the B cell compartment, whereas the percentage of T cells (both $CD4^+$ and $CD8^+$) was decreased (Fig. 5*B*). Percentages of macrophages and DC were increased in IMQ-treated mice. Additionally, an increase in the percentage of pDC was observed after IMQ treatment (Fig. 5*B*). This clearly shows that topical treatment of mice with IMQ results in systemic effects on the cellular composition of the spleen, with a shift from lymphoid to myeloid cells.

To determine the percentages of Th1, Th2, and Th17 cytokine-positive cells in the spleen, splenic cells were activated ex vivo by anti-CD3 for 4 h, stained intracellularly for IFN-γ, IL-4 and IL-17A, and analyzed using flow cytometry. IMQ-treated BALB/c mice showed an increased percentage of splenic $CD4^+$IL-$17A^+$IFN-γ^- T cells when compared with control-treated animals at day 5 (Fig. 6*A*). In contrast, the percentage of $CD4^+$IL-$17A^-$IFN-γ^+ T cells was hardly increased. Furthermore, almost no IL-17^+IFN-γ^+"double-positive" cells were found in IMQ-treated or control mice (Fig. 6*A*). Of interest, increased percentages of $CD4^+$IL-4^+ T cells were found in spleens of IMQ-treated mice when compared with the control group (Fig. 6*A*). Although some increase in the percentage of splenic $CD8^+$IL-$17A^+$ and $CD8^+$IL-4^+ T cells was detected, the percentages were relatively low compared with splenic $CD4^+$ T cells (Fig. 6*B*). In contrast, a marked increase for $CD8^+$IFN-γ^+ T cells was found after IMQ treatment (Fig. 6*B*). These data indicate systemic induction of Th17, Th2, and IFN-γ^+CD8^+ T cells after 5 days of IMQ treatment.

T cell deficiency results in significantly reduced IMQ-induced skin inflammation

Although it is generally accepted that T cells play an important role in the pathogenic process of human psoriasis (36), the differential contributions of functional and phenotypic subsets remain less clear.

To assess whether T cells are critical to IMQ-induced skin inflammation, we depleted $CD3^+$ T cells in vivo starting before IMQ application. The efficiency of the depletion was assayed by flow cytometry of the spleen cells of anti-CD3-treated mice. In control-treated mice, injection of anti-CD3 Abs resulted in ~70% reduction of the percentage of T cells of both $CD4^+$ and $CD8^+$ subsets, whereas in IMQ-treated mice, a 50% reduction of both $CD4^+$ and $CD8^+$ subsets occurred (Fig. 7*A*). These depletion efficacies are similar to the 50% reduction of splenic T cells that was reported previously using this Ab and a comparable depletion regimen (33).

Injection of depleting anti-CD3 Abs resulted in significantly decreased scores for inflammation of the back skin, as scored by independent observers blinded to treatment (Fig. 7*B*). All parameters of this score (erythema, scales, and thickness) were reduced (Fig. 7*C*). Moreover, also the IMQ-induced increase in ear thickness was significantly impaired upon depletion of $CD3^+$ cells (Fig. 7*D*). When skin samples from control- and IMQ-treated backs were analyzed for the presence of $CD3^+$ cells in situ, no clear effect of the CD3-depleting Ab was observed (data not shown). This indicates that although systemic depletion was successful, as demonstrated by flow cytometric analysis of spleens (Fig. 7*A*), most $CD3^+$ cells in the skin persisted. Despite this persistence, a consistent reduction of IMQ-induced skin inflammation was noted.

Furthermore, the functional role for T cells in IMQ-induced skin inflammation was assessed using $RAG2^{-/-}$common $\gamma^{-/-}$ mice that are completely devoid of T cells, B cells, NK cells, and NKT cells. Similarly to CD3-depleted mice, these immunodeficient mice showed a reduction in cumulative score of IMQ-induced skin inflammation of ~40% (Fig. 8*A*). Remarkably, in these mice not all individual parameters of skin inflammation (erythema, scales, and thickness) were affected equally (Fig. 8*A*). Additionally, the

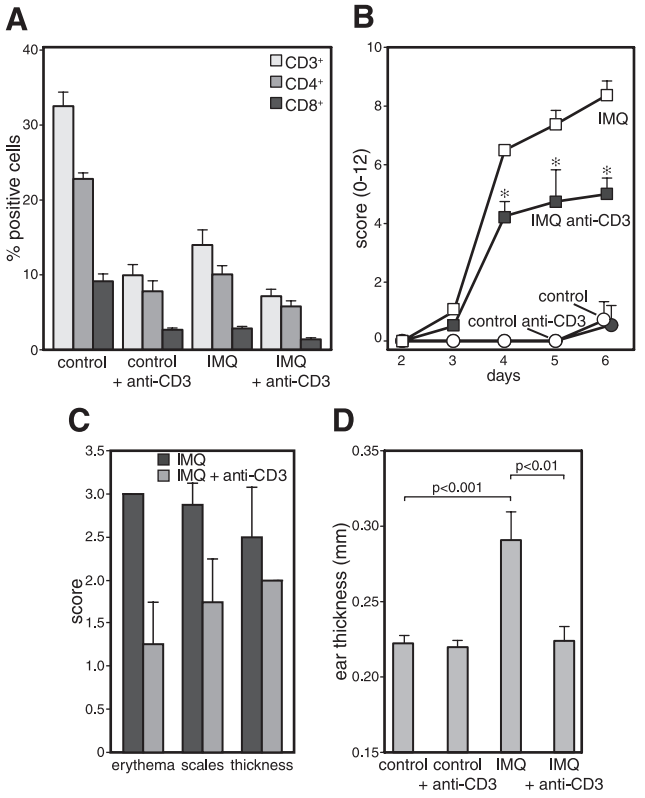

FIGURE 7. Depletion of $CD3^+$ cells attenuates IMQ-induced skin inflammation. Mice were treated daily with IMQ for 6 days and injected with anti-CD3 Abs at day −3, 0, and 3. *A*, Spleens were analyzed for the presence of $CD3^+$, $CD4^+$, and $CD8^+$ T cells. Erythema, scaling, and thickness of the back skin were scored daily. The cumulative score was calculated and depicted (*B*). Additionally, the parameters of skin inflammation (erythema, scaling, and thickness) at day 6 were depicted individually (*C*). Ear thickness of the right ear was measured on day 5 (*D*). Symbols represent mean score or ear thickness ± SD in two to four mice per group. Statistical significant differences ($p \leq 0.05$, Mann-Whitney *U* test) are indicated.

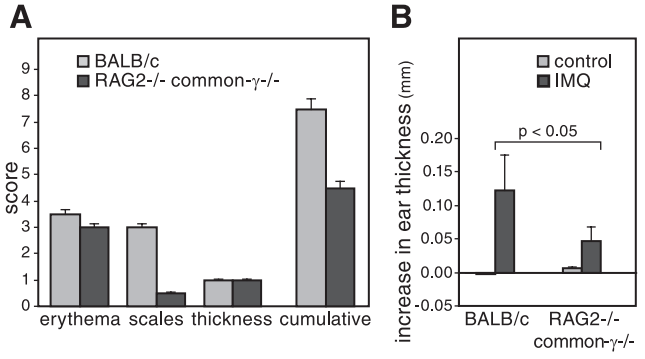

FIGURE 8. IMQ-induced skin inflammation is reduced in immunodeficient $RAG2^{-/-}$common $\gamma^{-/-}$ mice. $RAG2^{-/-}$common $\gamma^{-/-}$ and WT BALB/c mice were treated daily with IMQ for 6 days. *A*, Erythema, scaling, and thickness of the back skin were scored and depicted individually. Furthermore, the cumulative score was calculated. *B*, Ear thickness of the right ear was measured on day 1 and day 6, and the increase in ear thickness was calculated. Bars represent mean score or ear thickness ± SD in four mice per group.

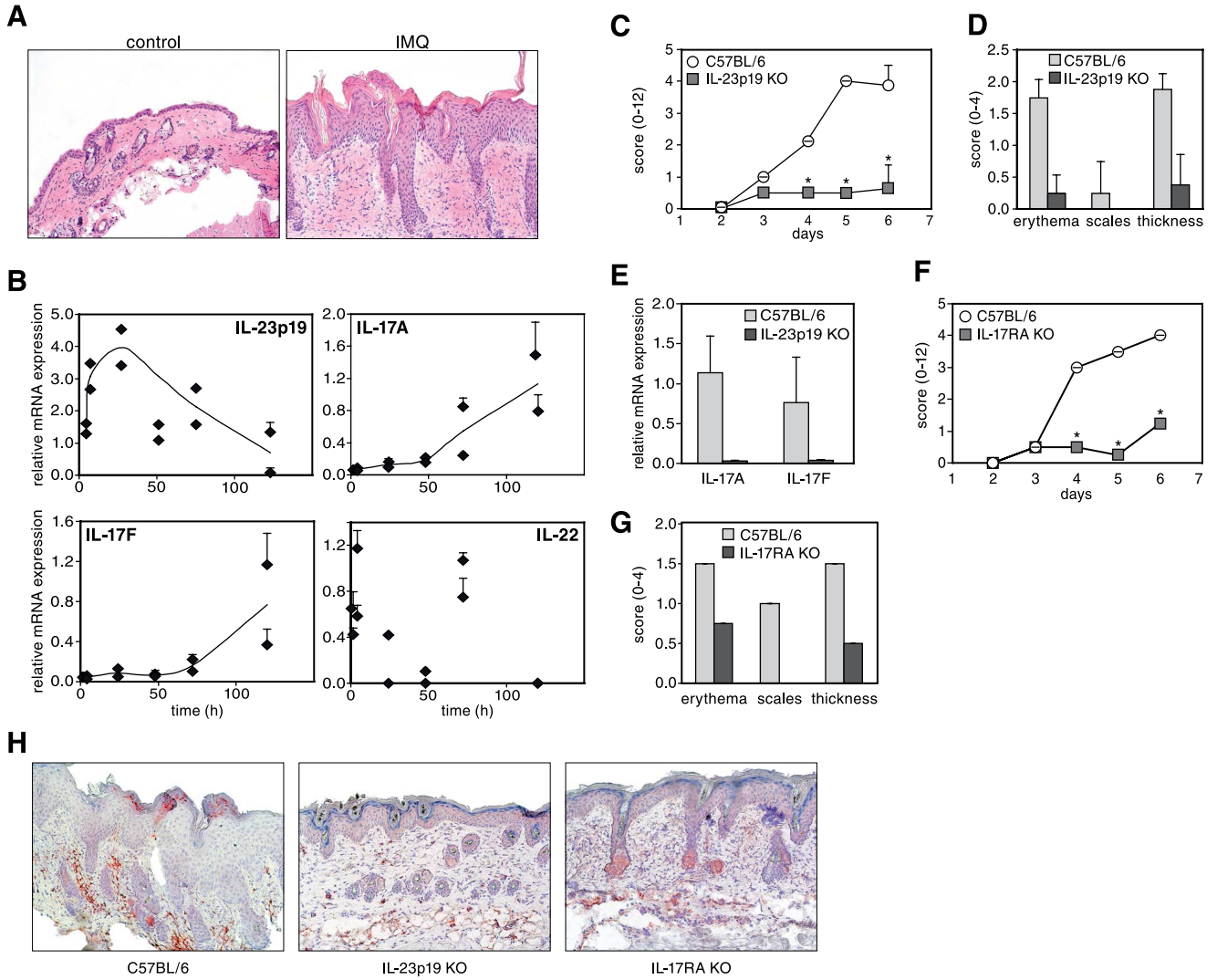

FIGURE 9. IMQ-induced skin inflammation is dependent on the IL-23/IL-17 axis. *A*, H&E staining of the back skin of C57BL/6 mice treated for 5 consecutive days with control cream or IMQ. *B*, RNA from back skin of C57BL/6 mice treated with IMQ for the time points indicated was analyzed for expression of IL-22, IL-23p19, IL-17A, and IL-17F by quantitative RT-PCR. Each symbol represents mRNA expression relative to GAPDH mRNA levels in an individual mouse, and a trend line, if present, is shown. C57BL/6, IL-23p19 KO, and IL-17RA KO mice were treated with IMQ for 5 days. Erythema, scaling, and thickness of the back skin were scored daily in C57BL/6 and IL-23p19 KO (*C* and *D*) or C57BL/6 and IL-17RA KO mice (*F* and *G*). The cumulative score (erythema plus scaling plus thickness) was calculated, indicated as mean ± SD of four mice per group, and significant differences ($p \leq 0.05$, Mann-Whitney *U* test) are indicated with asterisks (*C* and *F*). Additionally, the parameters of skin inflammation (erythema, scaling, and thickness) at day 6 were depicted individually as mean ± SD of four mice per group (*D* and *G*). *E*, IL-17A and IL-17F mRNA expression was determined in IMQ-treated C57BL/6 and IL-23p19 KO mice by quantitative RT-PCR. Bars indicate mean ± SD for two mice per group. *H*, Immunohistochemical staining for neutrophils (Gr1) was performed on back skin of C57BL/6, IL-23p19 KO, and IL-17RA KO mice treated for 5 days with IMQ.

ear swelling reaction was determined. Baseline ear thickness appeared different in wild-type (WT) BALB/c mice when compared with RAG2$^{-/-}$common $\gamma^{-/-}$ mice (0.216 ± 0.006 mm and 0.230 ± 0.007 mm, respectively). Nevertheless, ear swelling was significant reduced in RAG2$^{-/-}$common $\gamma^{-/-}$ mice (Fig. 8*B*).

In summary, in the absence of T cells, either by using CD3 depleting Abs or in T cell-deficient mice, IMQ-induced skin inflammation is partially blocked.

IMQ-induced skin inflammation is critically dependent on the IL-23/IL-17 axis

To assess a functional role the IL-23/IL-17 axis in the development of IMQ-induced skin inflammation, IL-23p19- and IL-17RA-deficient mice were used. Since these mice were on a C57BL/6 background, IMQ-induced skin inflammation was first assessed in C57BL/6 WT mice. In striking contrast to BALB/c mice, IMQ treatment had severe systemic effects in C57BL/6 mice, that is, mice became ill from day 2 of treatment onward, as evidenced by apathetic behavior and weight loss of ~15%, driving animals to become moribund. These effects might reflect a pyrogenic response and fever, since IMQ application transiently induced high levels of circulating IL-6 in C57BL/6, whereas no such increase was observed in BALB/c mice (data not shown). C57BL/6 mice could easily be rescued by just injecting 300 μl of PBS i.p. at day 3 and day 4.

Similarly, as observed for BALB/c mice, daily application of IMQ on the back of C57BL/6 mice resulted in erythema, scaling, and increased skin thickness. H&E-stained sections of IMQ-treated C57BL/6 skin demonstrated increased epidermal thickening (acanthosis) and a disturbed keratinocyte differentiation, as evidenced by retention of nuclei in the stratum corneum (parakeratosis) (Fig. 9*A*). Severity of IMQ-induced skin inflammation in C57BL/6 mice was consistently lower when compared

with BALB/c mice (Fig. 9, *C* and *F*, and Fig. 1*B*, respectively). IMQ application induced the expression of IL-23p19, IL-17A, and IL-17F in the back skin in C57BL/6 mice comparable to BALB/c, although with delayed kinetics (Fig. 9*B*). In contrast, IL-22 was not consistently induced by IMQ application on C57BL/6 (Fig. 9*B*), whereas a transient induction of IL-22 expression was observed in BALB/c mice. Immunohistochemical analyisis of IMQ-treated skin of C57BL/6 mice showed the presence of $Gr1^+$ neutrophils, both in the dermis as well as in microabscesses in the epidermis (Fig. 9*H*).

Application of control cream did not result in any signs of skin inflammation in IL-23p19-deficient, IL-17RA-deficient, or C57BL/6 WT mice (data not shown). IMQ-induced skin inflammation in IL-23p19-deficient mice resulted in substantially lower scores for erythema, scaling, and thickening (Fig. 9*D*), leading to a drastically reduced overall score in these mice compared with WT C57BL/6 mice (Fig. 9*C*). Since IL-23 is essential for Th17 survival and activity in vivo (37), we examined whether this IL-23/IL-17 axis is involved. Induction of IL-17A and IL-17F mRNA expression by IMQ application was completely abolished in IL-23p19-deficient mice (Fig. 9*E*). Interestingly, IMQ-induced skin inflammation in IL-17RA-deficient mice showed a similar profound suppression of erythema, scaling, and thickening as in the IL-23p19-deficient mice (Fig. 9, *F* and *G*). Histological analysis showed that epidermal thickening was markedly reduced in IMQ-treated IL-23p19- and IL-17RA-deficient mice, when compared with WT C57BL/6 mice (Fig. 9*H*). $Gr1^+$ microabscesses were not observed in the epidermis of IMQ-treated IL-23p19 or IL-17RA KO mice. Furthermore, the numbers of $Gr1^+$ neutrophils in the dermis were decreased 80–90% in IL-23p19 and IL-17RA KO mice, when compared with WT C57BL/6 mice (Fig. 9*H*).

Collectively, these data demonstrate the critical role of IL-23 in IMQ-induced skin inflammation. Furthermore, the downstream IL-17R signaling pathway is as pivotal for developing full-blown disease.

Discussion

Here we demonstrate that IMQ-treated mouse skin closely resembles human plaque-type psoriasis with respect to erythema, skin thickening, scaling, epidermal alterations (acanthosis, parakeratosis), and neoangiogenesis, as well as with respect to the inflammatory infiltrate consisting of T cells, neutrophils, DC, and pDC. Mechanistically, T cells are important for full-blown disease development, as reflected by anti-CD3 depletion treatment and the use of immunodeficient mice. Both IL-23 and IL-17 receptor signaling are absolutely critical to development of disease since genetic knockout of both molecules individually leads to a nearly complete blockade of disease, despite daily IMQ application during the entire 6-day experimental period.

This IMQ-induced skin inflammation model is based on application of a single synthetic innate Ag receptor ligand. Therefore, the model can be regarded as very clean in immunological terms since it does not require classical strong adjuvants like CFA or IFA. Hence, our data shed important new light on the Th1-Th17 conundrum, for which it has been argued very recently and eloquently that the use of CFA in autoimmune models of autoimmune disease might skew the importance of IL-17. This has led to the potentially premature conclusion that Th17 cells are the master mediators of tissue damage in several diseases, including psoriasis, multiple sclerosis, and rheumatoid arthritis (38). Nevertheless, a critical role for IL-17 has been demonstrated in spontaneous chronic inflammatory transgenic mouse models (39, 40).

Importantly, clinical topical use of IMQ for some weeks can unduly elicit psoriasis activity as a severe side effect, at the site of application but even at distant sites, speaking to this drug's systemic action (4–7). The IMQ skin model in mice helps to explain this phenomenon, and the very strong systemic effects of this synthetic compound are evidenced by the 2-fold increase in spleen mass (Fig. 5*A*).

Many mouse models for human psoriasis have been described, including spontaneous models, genetically engineered mice, and xenograft models. Extensive comparisons between these models have been made in various recent reviews (41–44). Nestle and Nickoloff (44) defined several criteria for an ideal psoriasis model: 1) epidermal changes based on keratinocyte hyperproliferation and altered differentiation; 2) papillomatosis (regular and symmetrical extension of rete ridges, separated by elongated dermal papillae); 3) presence of inflammatory cells including T cells, DC, and neutrophils; 4) a functional role for T cells; 5) altered vascularity; and 6) response to well-established antipsoriatic drugs. The models currently most closely resembling human psoriasis are xenograft models, where nonlesional psoriasis skin is transplanted onto immunodeficient SCID or AGR129 mice (18, 19). The results presented in our study show that IMQ-induced skin inflammation clearly and consistently fulfills criteria 1, 3, 4, and 5, whereas papillomatosis was sometimes, but not always, observed (criterion 2). Currently we are testing the therapeutic effect of well-established antipsoriasis drugs, such as cyclosporin A, corticosteroids, and anti-TNF-α, on the development of psoriasis-like skin inflammation in our model (criterion 6).

Criterion 4 above requires a functional role for T cells. Accordingly, we demonstrate that IMQ-induced skin inflammation was significantly attenuated, although evidently not completely abolished, in mice depleted for $CD3^+$ T cells or in immunodeficient $RAG2^{-/-}$common $\gamma^{-/-}$ mice (Figs. 7 and 8). In contrast, IMQ-induced skin inflammation was completely blocked in mice deficient for IL-23p19 or IL-17RA (Fig. 9), demonstrating a critical functional role for the IL-23/IL-17 axis in IMQ-induced skin inflammation. IL-17 can be produced by other cell types besides Th17 cells, including early responder T cells and nonleukocyte cell types. Since disease develops already within 3–5 days after application of IMQ as a single TLR ligand in the absence of additional classic adjuvant, innate immune mechanisms are evidently pivotal. Adaptive immunity requires at least 4 days to complete the cycle of Ag transport to the draining lymph node, APC-T cell interaction, clonal expansion, and finally re-migration of T cells to the skin to effect tissue damage driven by engagement of Ag-specific TCR. Thus, our data collectively suggest that both innate immune mechanisms and adaptive immunity contribute to the development of full-blown IMQ-induced skin inflammation.

A functional role for the IL-23/IL-17 axis in the pathogenesis of psoriasis was suggested recently. Intradermal injection of IL-23 in mouse skin induces several features of psoriatic skin such as erythema, an inflammatory infiltrate, and acanthosis (23, 24). Furthermore, therapeutic efficacy in psoriasis was shown for a mAb against the p40 subunit of IL-23 (25), leading to recent submission of this mAb to the Food and Drug Administration for market approval in the treatment of psoriasis. We therefore explored the IL-23/IL-17 axis in detail in the IMQ model. As shown in Fig. 9*C*, mice deficient for IL-23p19 are highly resistant to IMQ, underscoring the central role of this cytokine. Deficiency for the receptor for IL-17 has a similar strong effect, almost completely abolishing skin disease (Fig. 9, *F* and *G*). Previously it was shown that IL-23-induced acanthosis is dependent on the production of IL-22 by Th17 cells, rather than IL-17 (24). Flow cytometric analysis of spleen samples of IMQ-treated IL-23p19-deficient mice showed a lower percentage of $CD4^+IL\text{-}17A^+$ and $CD4^+IFN\text{-}\gamma^+$ T cells

when compared with WT mice, whereas no reduction in the percentage of $CD4^+IL\text{-}4^+$ cells was observed (data not shown). In contrast, in IMQ-treated IL-17RA deficient mice, no reduction in $CD4^+IL\text{-}17A^+$ T cell numbers occurred, whereas still a slightly lower percentage of $CD4^+IFN\text{-}\gamma^+$ T cells was noted (data not shown). Since these latter mice cannot signal for IL-17A and IL-17F, our data collectively suggest that IL-17A or IL-17F is at least one of the effector cytokines in IMQ-induced skin inflammation. Since IL-17A and IL-17F both signal via the IL-17RA, we cannot discriminate between these two cytokines of the IL-17 family, and further studies are needed using IL-17A- and IL-17F-specific KO mice to unravel this issue. IL-22 expression was increased in BALB/c mice, whereas no consistent increase was observed in C57BL/6 mice (Figs. 4 and 9*B*). Since C57BL/6 mice showed a reduced cumulative score of IMQ-induced skin inflammation, a role for IL-22 is plausible and deserves further investigation.

Some of the confusion on the role of IL-17 in (autoimmune) inflammatory diseases stems from the overlapping functions of IL-17A and IL-17F, as well as from the fact that many cell types are capable of secreting IL-17, implying that Th17 cells are only one of the sources. Furthermore, new functional T cell types are emerging, for instance with a mixed Th1-Th17 character ($CD4^+IFN\text{-}\gamma^+IL\text{-}17^+$"double positive"). Recently it has been shown that a relatively high percentage of γδ T cells produce IL-17A in autoimmune collagen-induced arthritis, a mouse model for human rheumatoid arthritis (45). IL-23 appeared to be critical for IL-17A production in these γδ T cells since IL-23-deficient mice showed a marked reduction of $IL\text{-}17A^+$ γδ T cells in experimental arthritis (F. Cornelissen, E. Lubberts, et al., manuscript in preparation). In the present study, we detected a higher percentage of $IL\text{-}17A^+$ γδ T cells in spleens of IMQ-treated BALB/c mice compared with control-treated mice (1.29% vs 0.26%, respectively, data not shown). In the mouse, >90% of the epidermal T cells are γδ-positive dendritic epidermal T cells (DETC). This subset plays an important role in skin homeostasis and during wound repair (reviewed in Ref. 46). Since psoriatic lesions share several factors with wound healing reactions (47), a pathogenic role for DETC in psoriasis is conceivable. Although in human epidermis no clear phenotypic equivalent of mice DETC has been identified, γδ-positive T cells do reside in the human dermis (48). Thus, further examination of the nature of the $CD3^+$ cells that are involved in the development of IMQ-induced skin inflammation in mice is mandatory.

A role for macrophages and/or pDC in the development of IMQ-induced psoriasis-like skin lesions is conceivable, since both of these cell types express TLR7 and are thus a potential target for IMQ. An essential role for macrophages was established recently in two different mouse models for psoriasis-like skin inflammation, that is, the CD18 hypomorphic PJ/L mice, and mice with an epidermis-specific deletion of IKK2 (49, 50). pDC play an essential role in the conversion of nonlesional to lesional psoriasis skin in a transplantation model (51). Based on the accumulation of pDC in IMQ-induced psoriatic skin lesions in humans, it was previously suggested that skin pDC are the primary targets for IMQ, leading to local increased type I IFN production (4). Additionally, IMQ induces the migration of LC to the draining lymph nodes, thereby increasing inflammatory reactions in mice (10). Therefore, in ongoing experiments we are further exploring the role of pDC by means of Ab depletion, as well as the potential involvement of LC employing conditional knockout mice (52).

In $RAG2^{-/-}$common $\gamma^{-/-}$ mice, not all parameters for skin inflammation (erythema, scales, and thickness) were attenuated equally when compared with WT mice (Fig. 8*A*). This can be explained by the differences in mechanisms involved in development of these parameters. Erythema represents the degree of vasodilatation in the dermis to which multiple cytokines (IL-1, TNF-α) and compounds (NO, phopholipase A_2 metabolites, histamine) from various cellular sources (keratinocytes, DC, mast cells) contribute. Skin thickness, or induration, is the result of increased keratinocyte proliferation, due to stimulation by proinflammatory cytokines, especially by IL-20 and IL-22, as well as dermal infiltration by inflammatory cells. Scaling reflects abnormal keratinocyte differentiation due to increased proliferation and the abnormal cytokine milieu. Thus, our model of IMQ-induced skin inflammation, in combination with depletion or deficiency of various cell types and/or cytokines, allows dissection of these distinct pathways contributing to skin inflammation.

In conclusion, we demonstrate that the skin lesions induced by topical application of IMQ closely resemble human psoriasis lesions. Furthermore, most criteria that are defined for a valid psoriasis mouse model are met. The model presented herein relies on a well-defined clinical therapeutic, develops fast (2–4 days) with 100% disease incidence, is highly robust with very little in-group and between-experiment variation, is effective in both Th1- and Th2-prone mouse strains (C57BL/6 and SJL/J vs BALB/c assessed), and requires limited facilities and experimental skills. Consequently, this system is also very suitable for a rapid first in vivo screening of potential antipsoriasis drugs.

Acknowledgments

The authors are grateful to Tar van Os for preparing the figures and Pieter Leenen for providing hybridoma culture supernatants for immunohistochemical stainings. Anne von Bergh and Rebecca Kiekens are thanked for technical assistance. We highly appreciate the kind gifts of the IL-23p19-deficient mice from Dr. N. Ghilardi (Genentech) and the IL-17RA-deficient mice from Dr. J. Tocker (Amgen).

Disclosures

The authors have no financial conflicts of interest.

References

1. Beutner, K. R., and S. Tyring. 1997. Human papillomavirus and human disease. *Am. J. Med.* 102: 9–15.
2. Szeimies, R. M., M. J. Gerritsen, G. Gupta, J. P. Ortonne, S. Serresi, J. Bichel, J. H. Lee, T. L. Fox, and A. Alomar. 2004. Imiquimod 5% cream for the treatment of actinic keratosis: results from a phase III, randomized, double-blind, vehicle-controlled, clinical trial with histology. *J. Am. Acad. Dermatol.* 51: 547–555.
3. Geisse, J. K., P. Rich, A. Pandya, K. Gross, K. Andres, A. Ginkel, and M. Owens. 2002. Imiquimod 5% cream for the treatment of superficial basal cell carcinoma: a double-blind, randomized, vehicle-controlled study. *J. Am. Acad. Dermatol.* 47: 390–398.
4. Gilliet, M., C. Conrad, M. Geiges, A. Cozzio, W. Thurlimann, G. Burg, F. O. Nestle, and R. Dummer. 2004. Psoriasis triggered by Toll-like receptor 7 agonist imiquimod in the presence of dermal plasmacytoid dendritic cell precursors. *Arch. Dermatol.* 140: 1490–1495.
5. Wu, J. K., G. Siller, and G. Strutton. 2004. Psoriasis induced by topical imiquimod. *Australas. J. Dermatol.* 45: 47–50.
6. Rajan, N., and J. A. Langtry. 2006. Generalized exacerbation of psoriasis associated with imiquimod cream treatment of superficial basal cell carcinomas. *Clin. Exp. Dermatol.* 31: 140–141.
7. Fanti, P. A., E. Dika, S. Vaccari, C. Miscial, and C. Varotti. 2006. Generalized psoriasis induced by topical treatment of actinic keratosis with imiquimod. *Int. J. Dermatol.* 45: 1464–1465.
8. Palamara, F., S. Meindl, M. Holcmann, P. Luhrs, G. Stingl, and M. Sibilia. 2004. Identification and characterization of pDC-like cells in normal mouse skin and melanomas treated with imiquimod. *J. Immunol.* 173: 3051–3061.
9. Schon, M. P., and M. Schon. 2007. Imiquimod: mode of action. *Br. J. Dermatol.* 157(Suppl. 2): 8–13.
10. Suzuki, H., B. Wang, G. M. Shivji, P. Toto, P. Amerio, M. A. Tomai, R. L. Miller, and D. N. Sauder. 2000. Imiquimod, a topical immune response modifier, induces migration of Langerhans cells. *J. Invest. Dermatol.* 114: 135–141.
11. Gibson, S. J., J. M. Lindh, T. R. Riter, R. M. Gleason, L. M. Rogers, A. E. Fuller, J. L. Oesterich, K. B. Gorden, X. Qiu, S. W. McKane, et al. 2002. Plasmacytoid dendritic cells produce cytokines and mature in response to the TLR7 agonists, imiquimod and resiquimod. *Cell. Immunol.* 218: 74–86.
12. Wagner, T. L., C. L. Ahonen, A. M. Couture, S. J. Gibson, R. L. Miller, R. M. Smith, M. J. Reiter, J. P. Vasilakos, and M. A. Tomai. 1999. Modulation

of TH1 and TH2 cytokine production with the immune response modifiers, R-848 and imiquimod. *Cell Immunol.* 191: 10–19.
13. Fujisawa, H., G. M. Shivji, S. Kondo, B. Wang, M. A. Tomai, R. L. Miller, and D. N. Sauder. 1996. Effect of a novel topical immunomodulator, S-28463, on keratinocyte cytokine gene expression and production. *J. Interferon Cytokine Res.* 16: 555–559.
14. Kono, T., S. Kondo, S. Pastore, G. M. Shivji, M. A. Tomai, R. C. McKenzie, and D. N. Sauder. 1994. Effects of a novel topical immunomodulator, imiquimod, on keratinocyte cytokine gene expression. *Lymphokine Cytokine Res.* 13: 71–76.
15. Kollisch, G., B. N. Kalali, V. Voelcker, R. Wallich, H. Behrendt, J. Ring, S. Bauer, T. Jakob, M. Mempel, and M. Ollert. 2005. Various members of the Toll-like receptor family contribute to the innate immune response of human epidermal keratinocytes. *Immunology* 114: 531–541.
16. Lebre, M. C., A. M. van der Aar, L. van Baarsen, T. M. van Capel, J. H. Schuitemaker, M. L. Kapsenberg, and E. C. de Jong. 2007. Human keratinocytes express functional Toll-like receptor 3, 4, 5, and 9. *J. Invest. Dermatol.* 127: 331–341.
17. Schon, M. P., M. Schon, and K. N. Klotz. 2006. The small antitumoral immune response modifier imiquimod interacts with adenosine receptor signaling in a TLR7- and TLR8-independent fashion. *J. Invest. Dermatol.* 126: 1338–1347.
18. Boyman, O., H. P. Hefti, C. Conrad, B. J. Nickoloff, M. Suter, and F. O. Nestle. 2004. Spontaneous development of psoriasis in a new animal model shows an essential role for resident T cells and tumor necrosis factor-α. *J. Exp. Med.* 199: 731–736.
19. Wrone-Smith, T., and B. J. Nickoloff. 1996. Dermal injection of immunocytes induces psoriasis. *J. Clin. Invest.* 98: 1878–1887.
20. Lee, E., W. L. Trepicchio, J. L. Oestreicher, D. Pittman, F. Wang, F. Chamian, M. Dhodapkar, and J. G. Krueger. 2004. Increased expression of interleukin 23 p19 and p40 in lesional skin of patients with psoriasis vulgaris. *J. Exp. Med.* 199: 125–130.
21. Piskin, G., R. M. Sylva-Steenland, J. D. Bos, and M. B. Teunissen. 2006. In vitro and in situ expression of IL-23 by keratinocytes in healthy skin and psoriasis lesions: enhanced expression in psoriatic skin. *J. Immunol.* 176: 1908–1915.
22. Lowes, M. A., T. Kikuchi, J. Fuentes-Duculan, I. Cardinale, L. C. Zaba, A. S. Haider, E. P. Bowman, and J. G. Krueger. 2008. Psoriasis vulgaris lesions contain discrete populations of Th1 and Th17 T cells. *J. Invest. Dermatol.* 128: 1207–1211.
23. Chan, J. R., W. Blumenschein, E. Murphy, C. Diveu, M. Wiekowski, S. Abbondanzo, L. Lucian, R. Geissler, S. Brodie, A. B. Kimball, et al. 2006. IL-23 stimulates epidermal hyperplasia via TNF and IL-20R2-dependent mechanisms with implications for psoriasis pathogenesis. *J. Exp. Med.* 203: 2577–2587.
24. Zheng, Y., D. M. Danilenko, P. Valdez, I. Kasman, J. Eastham-Anderson, J. Wu, and W. Ouyang. 2007. Interleukin-22, a T_H17 cytokine, mediates IL-23-induced dermal inflammation and acanthosis. *Nature* 445: 648–651.
25. Krueger, G. G., R. G. Langley, C. Leonardi, N. Yeilding, C. Guzzo, Y. Wang, L. T. Dooley, and M. Lebwohl. 2007. A human interleukin-12/23 monoclonal antibody for the treatment of psoriasis. *N. Engl. J. Med.* 356: 580–592.
26. Haider, A. S., M. A. Lowes, M. Suarez-Farinas, L. C. Zaba, I. Cardinale, A. Khatcherian, I. Novitskaya, K. M. Wittkowski, and J. G. Krueger. 2008. Identification of cellular pathways of "type 1," Th17 T cells, and TNF- and inducible nitric oxide synthase-producing dendritic cells in autoimmune inflammation through pharmacogenomic study of cyclosporine A in psoriasis. *J. Immunol.* 180: 1913–1920.
27. Zaba, L. C., I. Cardinale, P. Gilleaudeau, M. Sullivan-Whalen, F. M. Suarez, J. Fuentes-Duculan, I. Novitskaya, A. Khatcherian, M. J. Bluth, M. A. Lowes, and J. G. Krueger. 2007. Amelioration of epidermal hyperplasia by TNF inhibition is associated with reduced Th17 responses. *J. Exp. Med.* 204: 3183–3194.
28. Bos, J. D. 2007. Psoriasis, innate immunity, and gene pools. *J. Am. Acad. Dermatol.* 56: 468–471.
29. Hollox, E. J., U. Huffmeier, P. L. Zeeuwen, R. Palla, J. Lascorz, D. Rodijk-Olthuis, P. C. van de Kerkhof, H. Traupe, G. de Jongh, M. den Heijer, et al. 2008. Psoriasis is associated with increased β-defensin genomic copy number. *Nat. Genet.* 40: 23–25.
30. Ghilardi, N., N. Kljavin, Q. Chen, S. Lucas, A. L. Gurney, and F. J. de Sauvage. 2004. Compromised humoral and delayed-type hypersensitivity responses in IL-23-deficient mice. *J. Immunol.* 172: 2827–2833.
31. Ye, P., F. H. Rodriguez, S. Kanaly, K. L. Stocking, J. Schurr, P. Schwarzenberger, P. Oliver, W. Huang, P. Zhang, J. Zhang, et al. 2001. Requirement of interleukin 17 receptor signaling for lung CXC chemokine and granulocyte colony-stimulating factor expression, neutrophil recruitment, and host defense. *J. Exp. Med.* 194: 519–527.
32. Wils, E. J., E. Braakman, G. M. Verjans, E. J. Rombouts, A. E. Broers, H. G. Niesters, G. Wagemaker, F. J. Staal, B. Lowenberg, H. Spits, and J. J. Cornelissen. 2007. Flt3 ligand expands lymphoid progenitors prior to recovery of thymopoiesis and accelerates T cell reconstitution after bone marrow transplantation. *J. Immunol.* 178: 3551–3557.
33. Mysliwietz, J., and S. Thierfelder. 1992. Antilymphocytic antibodies and marrow transplantation: XII. Suppression of graft-versus-host disease by T-cell-modulating and depleting antimouse CD3 antibody is most effective when preinjected in the marrow recipient. *Blood* 80: 2661–2667.
34. van der Fits, L., L. I. van der Wel, J. D. Laman, E. P. Prens, and M. C. Verschuren. 2004. In psoriasis lesional skin the type I interferon signaling pathway is activated, whereas interferon-α sensitivity is unaltered. *J. Invest. Dermatol.* 122: 51–60.
35. Asselin-Paturel, C., G. Brizard, J. J. Pin, F. Briere, and G. Trinchieri. 2003. Mouse strain differences in plasmacytoid dendritic cell frequency and function revealed by a novel monoclonal antibody. *J. Immunol.* 171: 6466–6477.
36. Gudjonsson, J. E., A. Johnston, H. Sigmundsdottir, and H. Valdimarsson. 2004. Immunopathogenic mechanisms in psoriasis. *Clin. Exp. Immunol.* 135: 1–8.
37. Veldhoen, M., R. J. Hocking, C. J. Atkins, R. M. Locksley, and B. Stockinger. 2006. TGFβ in the context of an inflammatory cytokine milieu supports de novo differentiation of IL-17-producing T cells. *Immunity* 24: 179–189.
38. Steinman, L. 2008. A rush to judgment on Th17. *J. Exp. Med.* 205: 1517–1522.
39. Nakae, S., S. Saijo, R. Horai, K. Sudo, S. Mori, and Y. Iwakura. 2003. IL-17 production from activated T cells is required for the spontaneous development of destructive arthritis in mice deficient in IL-1 receptor antagonist. *Proc. Natl. Acad. Sci. USA* 100: 5986–5990.
40. Hirota, K., M. Hashimoto, H. Yoshitomi, S. Tanaka, T. Nomura, T. Yamaguchi, Y. Iwakura, N. Sakaguchi, and S. Sakaguchi. 2007. T cell self-reactivity forms a cytokine milieu for spontaneous development of IL-17$^+$ Th cells that cause autoimmune arthritis. *J. Exp. Med.* 204: 41–47.
41. Schon, M. P. 1999. Animal models of psoriasis: what can we learn from them? *J. Invest. Dermatol.* 112: 405–410.
42. Gudjonsson, J. E., A. Johnston, M. Dyson, H. Valdimarsson, and J. T. Elder. 2007. Mouse models of psoriasis. *J. Invest. Dermatol.* 127: 1292–1308.
43. Mizutani, H., K. Yamanaka, H. Konishi, and T. Murakami. 2003. Animal models of psoriasis and pustular psoriasis. *Arch. Dermatol. Res.* 295(Suppl. 1): 67–68.
44. Nestle, F. O., and B. J. Nickoloff. 2006. Animal models of psoriasis: a brief update. *J. Eur. Acad. Dermatol. Venereol.* 20(Suppl. 2): 24–27.
45. Roark, C. L., J. D. French, M. A. Taylor, A. M. Bendele, W. K. Born, and R. L. O'Brien. 2007. Exacerbation of collagen-induced arthritis by oligoclonal, IL-17-producing $\gamma\delta$ T cells. *J. Immunol.* 179: 5576–5583.
46. Jameson, J., and W. L. Havran. 2007. Skin $\gamma\delta$ T-cell functions in homeostasis and wound healing. *Immunol. Rev.* 215: 114–122.
47. Nickoloff, B. J., B. K. Bonish, D. J. Marble, K. A. Schriedel, L. A. DiPietro, K. B. Gordon, and M. W. Lingen. 2006. Lessons learned from psoriatic plaques concerning mechanisms of tissue repair, remodeling, and inflammation. *J. Investig. Dermatol. Symp. Proc.* 11: 16–29.
48. Holtmeier, W., M. Pfander, A. Hennemann, T. M. Zollner, R. Kaufmann, and W. F. Caspary. 2001. The TCR-δ repertoire in normal human skin is restricted and distinct from the TCR-δ repertoire in the peripheral blood. *J. Invest. Dermatol.* 116: 275–280.
49. Stratis, A., M. Pasparakis, R. A. Rupec, D. Markur, K. Hartmann, K. Scharffetter-Kochanek, T. Peters, N. van Rooijen, T. Krieg, and I. Haase. 2006. Pathogenic role for skin macrophages in a mouse model of keratinocyte-induced psoriasis-like skin inflammation. *J. Clin. Invest.* 116: 2094–2104.
50. Wang, H., T. Peters, D. Kess, A. Sindrilaru, T. Oreshkova, N. van Rooijen, A. Stratis, A. C. Renkl, C. Sunderkotter, M. Wlaschek, et al. 2006. Activated macrophages are essential in a murine model for T cell-mediated chronic psoriasiform skin inflammation. *J. Clin. Invest.* 116: 2105–2114.
51. Nestle, F. O., C. Conrad, A. Tun-Kyi, B. Homey, M. Gombert, O. Boyman, G. Burg, Y. J. Liu, and M. Gilliet. 2005. Plasmacytoid predendritic cells initiate psoriasis through interferon-α production. *J. Exp. Med.* 202: 135–143.
52. Bennett, C. L., and B. E. Clausen. 2007. DC ablation in mice: promises, pitfalls, and challenges. *Trends Immunol.* 28: 525–531.